Stacking Ensemble Learning for Non-Line-of-Sight Detection of Global Navigation Satellite System

Yuan Sun and Li Fu

***Abstract*— While the global navigation satellite system (GNSS) has been widely used to provide high-precision location services in many applications, it usually suffers from performance degradation due to non-line-of-sight (NLOS) reception. As the received NLOS signals might have great measurement errors especially in urban canyons, they should be detected to mitigate the errors contaminating the positioning systems. However, the NLOS detection is quite challenging as the accuracy rate is usually highly related to the surrounding environment the receiver is located in. To address this problem, we propose a stacking ensemble learning (SEL) method for the NLOS detection of GNSS. First, satellite measurement features are extracted from the GNSS raw measurements via a designed data processing module. Then, they are input to the SEL module consisting of two levels of machine learning models. In the first level, a support vector machine (SVM) and an extreme gradient boosting (XGBoost) are adopted in parallel, and the outputs of the fist-level models are input to the second-level logistic regression (LR) to obtain NLOS predictions. The proposed SEL module combines the views of different models to the measurement features to address the shortcomings of each single model and improve the model's generalization. Experimental results on real GNSS observations in urban canyons show that the proposed method outperforms the baseline machine learning methods with obvious detection accuracy improvements.**

***Index Terms*— Ensemble learning, global navigation satellite system (GNSS), machine learning, non-line-of-sight (NLOS).**

I. Introduction

RECENTLY, the global navigation satellite system (GNSS) is playing an increasingly important role in a wide range of applications, such as intelligent transportation system (ITS) [1], [2], location-based service (LBS) [3], and artificial intelligence of things (AIoT) [4]. Nevertheless, the GNSS positioning could exhibit a serious error caused by the notorious non-line-of-sight (NLOS) reception [5]–[7], especially in urban environments—the direct line-of-sight (LOS) signal is blocked while the signal is received only via reflections. As the reflected GNSS signal is propagated through an extra path than the corresponding direct LOS signal that the user does not receive, it will introduce a bias in the GNSS pseudorange measurement and cause a significant performance degradation [8]. Thus, to improve the accuracy of GNSS receivers, NLOS signals should be countered for the positioning system.

To address this issue, a natural idea is to detect NLOS from all GNSS signals and then eliminate it prior to the position calculation. However, the NLOS detection of GNSS is always a challenge problem, due to it being closely related to the environment surroundings of the user [9]. On the one hand, the environment might be complicated with different structures of buildings or trees, while NLOS signals might vary in different environments and can be difficult to model for detection. On the other hand, different from the multipath effect [10] that the GNSS user receives both reflected and direct signals at the same time, the user in NLOS reception phenomena does not receive the direct LOS signal of a satellite but only receives its reflected pattern. Thus, it is challenging to detect NLOS without a reference of the corresponding LOS signal.

A variety of studies on the NLOS detection of GNSS have been conducted in the navigation domain. Typically, GNSS measurement features [11] that consist of raw measurements and/or the quantities calculated from the measurements are used for NLOS detection. Related work can be divided into three categories according to how to use measurement features.

1) Single measurement feature of GNSS signals is used to detect NLOS.
2) A combination of multiple measurement features of GNSS signals are used to detect NLOS.
3) A combination of multiple measurement features of GNSS signals and other sensors are used to detect NLOS.

As for the first category, simple satellite measurements are usually adopted to directly detect NLOS signals via comparison with an empirical threshold. The measurements include carrier-to-noise ratio C/N_0 and satellite elevation angle [12]. However, the strategies based on the simple measurements would not work as the NLOS signals might not follow the expected behavior. For example, the strong reflection of GNSS signals with high C/N_0 will result in detection missing, and the satellites with low elevation angles might not be blocked by surrounding buildings [13].

To address the shortage of single measurement, the second category of studies focuses on using multiple satellite measurements to better distinguish NLOS and LOS signals. Considering the excellent performance of machine learning

Manuscript received February 9, 2022; revised March 27, 2022; accepted April 19, 2022. Date of publication April 28, 2022; date of current version May 9, 2022. This work was supported in part by the National Natural Science Foundation of China under Grant 61803037. The Associate Editor coordinating the review process was Dr. Alessio De Angelis. *(Corresponding author: Yuan Sun.)*

Yuan Sun is with the School of Electronic Engineering, Beijing University of Posts and Telecommunications, Beijing 100876, China (e-mail: sunyuan@bupt.edu.cn).

Li Fu is with JD AI Research, Beijing 100176, China (e-mail: fouri_er@126.com).

Digital Object Identifier 10.1109/TIM.2022.3170985

in detection and classification tasks, more work about how to use machine learning to improve the detection performance of NLOS has been proposed. Hsu [14] adopted a support vector machine (SVM) to an LOS/NLOS classification task based on multiple measurement features, including the difference between delta pseudorange and pseudorange rate. Sun *et al.* [15] used the three measurement features of C/N_0, pseudorange residuals, and satellite elevation angle with a gradient boosting decision tree (GBDT)-based classification algorithm and achieved significant improvement in NLOS detection rate. Zhang *et al.* [16] compared different machine learning methods, including SVM, K-nearest neighbors (KNN), neural network (NN), and decision tree (DT) on NLOS detection. In their work, the experimental results showed that the SVM outperformed other methods in different urban scenarios. Xu *et al.* [11] also extended the measurement features for SVM using signal-to-noise ratio (SNR), pseudorange, elevation angle, and so on.

Regarding the methods of the third category, extra sensors are applied as aids to improve the performance of GNSS NLOS detection. For example, a fish-eye camera was applied to detect the borderline between the sky and the obstacles from the colored fish-eye image to exclude NLOS satellites [17]. A fish-eye camera was also adopted to generate a visibility mask to improve the detection of NLOS [18]. Another method is using the 3-D light detection and ranging (LiDAR) to provide surrounding environment obstacles to the user and detect the NLOS signal [19], [20]. However, performance of these methods relies on the image processing, which might be unstable to illumination conditions or weather conditions.

Besides the detection scheme, NLOS mitigation is another widely studied solution, which aims to directly reduce the GNSS positioning errors caused by NLOS reception. The existing mitigation methods for GNSS signals can be divided into hardware-based methods and methods based on data processing [5]. First, as for the hardware-based methods, the choke-ring antenna-based method is usually used to give low gains to low elevation satellites and mitigate the effect of reflected GNSS signals [21]. However, as referred in [22], the method exhibits little protection against reflected signals with higher elevation. Receiver-based methods also belong to the hardware-based methods, such as delay lock loop [23], [24], which separates LOS and reflected signals via feedback loop. Nevertheless, the method might suffer from performance degradation when the direct LOS is blocked in NLOS reception phenomena. Second, considering the high cost and inconvenience of hardware updating, NLOS mitigation methods based on data processing attract more attention in the navigation domain. For example, the measurements of C/N_0 and elevation angle were used for weighting adjustment positioning via downweighting the effect of NLOS signals [25], [26]. However, as mentioned in the first category of the detection methods, the performance might be unstable, because the two measurements of NLOS vary greatly in different environments. Alternatively, based on the assumption that NLOS measurements produce a less consistent pseudorange residual or navigation solution, consistency checking techniques were explored for NLOS mitigation [27]–[29]. However, the performance of consistency checking will meet challenges when a large proportion of the signals are NLOS or multipath contaminated [22].

By comparing with the mitigation and detection methods for GNSS NLOS mentioned earlier, the main advantage of detection methods is that they could eliminate the contaminated measurements prior to the position calculation. Ideally, with a much larger choice of signals from multi-constellation GNSS, optimal position results might be obtained by selecting only those signals least contaminated by NLOS and excluding the rest [25].

However, in the existing works of NLOS detection, more effort is paid on measurement feature selection in GNSS signals or other sensors, and the machine learning model adopted to detect NLOS is usually a simple version. In practice, these existing methods using a single model may fall into a local optimal solution [30]. As the NLOS detection of GNSS is highly dependent on the surroundings, the existing machine learning models might not have a good generalization to the environment. To alleviate this problem, stacking ensemble learning (SEL) has shown great potential via blending different and heterogeneous base models with particular parameters to reduce the bias of each single model and decrease the generalization error [31]. In this article, we proposed an SEL for the NLOS detection of GNSS to further improve the performance of GNSS positioning. The proposed SEL consists of two levels of different machine learning models. It comprehensively considers the processing results of different first-level machine learning models on all of these features and makes the final decision of NLOS detection via a second-level machine learning model. The main advantage of SEL is that it combines different machine learning methods from different views to address the shortcomings of each single model. Experimentally, as for NLOS detection tasks of GNSS, the proposed SEL significantly improves the detection accuracy in comparison with the baseline machine learning methods. The main contributions of our work are shown as follows.

1) To the best of our knowledge, this is the first work using SEL for the NLOS detection of GNSS.
2) We propose a new SEL method for the NLOS detection of GNSS to fuse different models' advantages on detection tasks.
3) We evaluate the effectiveness of our method with real GNSS observation data, and our method significantly outperforms the baseline machine learning methods with obvious detection accuracy improvements.

The remainder of this article is organized as follows. Section II is the details of the proposed SEL for NLOS detection of GNSS, including the descriptions of measurement features used for detection and the proposed SEL method. Section III shows the experimental results and discussion. Finally, the conclusions and future work are given in Section IV.

II. Proposed Method

In this section, the proposed SEL for NLOS detection of GNSS is explained in detail. First, the system architecture of the proposed method is presented. Then, the data process

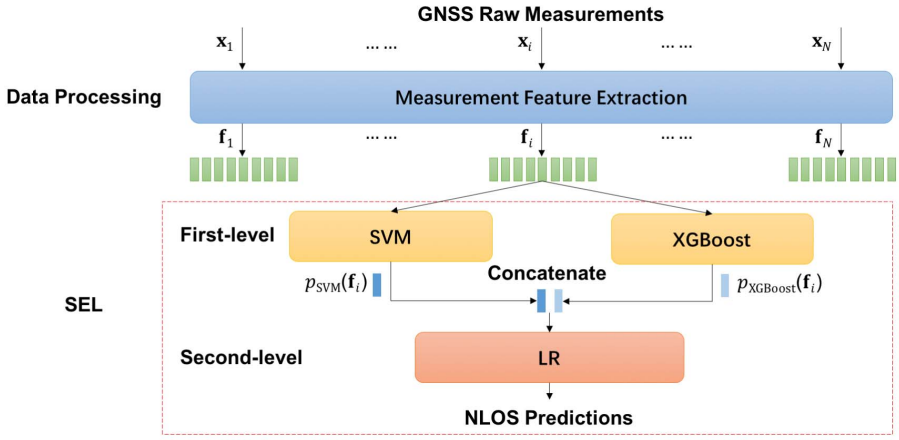

Fig. 1. System architecture of the proposed SEL for NLOS detection of GNSS, which mainly consists of the data processing and SEL.

of measurement feature extraction is designed for machine learning. Finally, the ensemble learning method is proposed for GNSS NLOS detection.

A. System Architecture

The goal of this article is to develop an NLOS detection method for GNSS measurements of a receiver. To achieve this, a method based on SEL is proposed, which combines different machine learners to improve the prediction results than each individual model. The system architecture of the proposed SEL for NLOS detection of GNSS is shown in Fig. 1, which mainly consists of two modules, i.e., data processing and SEL, as follows.

First, the received GNSS raw measurements $\{\mathbf{x}_i | i \in N\}$ of a receiver are input to the data processing module, with N the number of received GNSS satellites at a sampling time. In this article, the extracted measurement features $\mathbf{f} \in \mathbf{R}^9$ of a observed satellite are a 9-D vector, which consists of pseudorange $p \in \mathbf{R}$, SNR $s_n \in \mathbf{R}$, elevation angle $e \in \mathbf{R}$, azimuth angle $a \in \mathbf{R}$, pseudorange residual $p_r \in \mathbf{R}$, pseudorange rate consistency $p_{\mathrm{rc}} \in \mathbf{R}$, and satellite positions $\mathbf{s} \in \mathbf{R}^3$. More of other features will be further researched in our future work.

Then, the measurement features of each satellite are input to the proposed SEL module, which consists of two levels of different machine learning models. In practice, there are many individual models that can be adopted into the first and second levels of the SEL framework.[1] Empirically, in the first level, we consider three state-of-the-art machine learning models, i.e., SVM, extreme gradient boosting (XGBoost), and random forest (RF) [32]. All of these models are widely and successfully used in many real applications. As for the second level, we experiment with the widely used logistic regression (LR) and XGBoost to ensemble the prediction outputs of the first level. To make a balance between the final accuracy and the computational cost, in our method, there are two individual first-level machine learning models, i.e., SVM [33] and XGBoost [34]. Then, the prediction results of these first-level models are concatenated and input to the second-level LR [35]. The choice of these machine learning models will be tested in Section III. Note that these models of the proposed method are trained on a training dataset. By combining the outputs of different models, the SEL module outputs the final NLOS predictions of each received satellite.

[1]The individual models in ensemble learning can also be ensemble learners.

TABLE I

EXTRACTED MEASUREMENT FEATURES OF A VISIBLE SATELLITE FOR GNSS NLOS DETECTION, WHICH CONSIST OF THE GNSS RAW MEASUREMENTS (R) AND MEASUREMENT FEATURES VIA DATA PROCESSING (P)

Features	Symbols	Dimension	R/P
Signal to Noise Ratio	s_n	1	R
Pseudorange	p	1	
Satellite Positions	$\mathbf{s}$	3	
Elevation Angle	e	1	P
Azimuth Angle	a	1	
Pseudorange Residual	p_r	1	
Pseudorange Rate Consistency	p_{rc}	1	

B. Data Processing

Measurement feature is an important premise in determining the machine learning performance. In this section, our purpose is to design a data processing modular to obtain measurement features input to the followed SEL modular and improve the NLOS detection accuracy. The selected measurement features $\mathbf{f}$ consist of the GNSS raw measurements and its simple processing, as shown in Table I. The raw GNSS measurements include SNR s_n, pseudorange p, and satellite positions $\mathbf{s} = \{s_1, s_2, s_3\}$, where s_1, s_2, and s_3 are the three dimension positions of a visible satellite in the Earth-centered Earth-fixed (ECEF) coordinate system, respectively. Nevertheless, empirically, the relation between such raw measurements and NLOS can be hard to model [36]. Thus, based on the raw measurement, we add some measurement features that may be more relevant to NLOS by performing some simple data processing methods. These features include elevation angle e, azimuth angle a, pseudorange residual p_r, and pseudorange rate consistency p_{rc}. Overall, the 9-D measurement feature vector can be obtained for each satellite signal at a sampling

time. The calculation details for these quantities via data processing are shown as follows.

1) *Elevation Angle*: The satellite elevation angle e can be estimated by $e = \sin^{-1}(\widehat{\mathbf{r}}_U/\|\widehat{\mathbf{r}}\|)$, where $\widehat{\mathbf{r}} \in \mathbf{R^3}$ is the estimated satellite position in the east-north-up (ENU) coordinate system with respect to the receiver's position, with $\widehat{\mathbf{r}}_E$, $\widehat{\mathbf{r}}_N$, and $\widehat{\mathbf{r}}_U$ the "East," "North," and "Up" components, respectively. As the receiver's positioning error is negligible compared with the distance between the satellite and the receiver, the satellite elevation angle can be estimated with an acceptable accuracy using the estimated measurements [15].
2) *Azimuth Angle*: Similar to the calculation of the elevation angle, the satellite's azimuth angle a can be calculated by $a = \tan^{-1}(\widehat{\mathbf{r}}_E/\widehat{\mathbf{r}}_N)$.
3) *Pseudorange Residual*: The pseudorange residual p_r is the satellite's corresponding item of the estimated pseudorange residual vector $\epsilon = \triangle\rho - \mathbf{H}(\mathbf{H}^T\mathbf{H})^{-1}\mathbf{H}^T \triangle \rho$, where $\triangle\rho \in \mathbf{R}^N$ is the difference between the pseudorange measurements and the geometric distances from the estimated receiver position to the satellites; $\mathbf{H}$ is the satellite geometry matrix [11].
4) *Pseudorange Rate Consistency*: The pseudorange rate consistency p_{rc} can be estimated by $p_{\text{rc}} = p_D - p_p$, where p_p is the difference between the pseudorange measurements of two adjacent epoches, and $p_D = -\lambda f_D \triangle t$ is the pseudorange rate from Doppler shift with λ the carrier wavelength, f_D the Doppler shift measurement of the satellite, and $\triangle t$ the interval of two adjacent epoches.

C. SEL Method

As discussed in Section I, ensemble learning is adopted to combine several individual models to obtain better performance of NLOS detection under different environments. In general, the models of the proposed method are trained and evaluated on the training dataset $\boldsymbol{D}_t$ and the evaluation dataset $\boldsymbol{D}_e$, respectively.

Given the training dataset $\boldsymbol{D}_t$ consists of feature-label pairs $\{\mathbf{f}_t, y_t\}$, with $y_t \in \{0, 1\}$ the label of the measurement feature sample $\mathbf{f}_t$, the proposed SEL method is to train a model that can classify the NLOS ($y_t = 1$) and LOS ($y_t = 0$) of GNSS signals with a high accuracy. Similarly, the feature-label pairs of the evaluation dataset $\boldsymbol{D}_e$ can be denoted as $\{\mathbf{f}_e, y_e\}$. In particular, a two-level SEL method is proposed to combine heterogeneous weak models to produce a strong model that is less biased than its component weak models. In the first level, several models are combined in parallel to output different weak model predictions from different views. In the second level, there is a machine learning model, which is trained to output the final prediction based on the predictions of the first level.

Various combination strategies of basic machine learners can be selected to the SEL method, while the method needs to make a balance between the final accuracy and the computational cost. In the proposed SEL method for GNSS NLOS detection, the first-level models are two state-of-the-art machine learning methods, including SVM [11] and XGBoost [34]. Then, the predictions of these first-level models are concatenated and input to the second-level LR. A brief introduction to the principles of the selected machine learning models is provided as follows.

First-Level Model ①—SVM: The SVM performs structural risk minimization instead of minimizing the absolute value of an error, which addresses the overfitting issues by balancing the model's complexity against its success at fitting the training data. It has also been proved to be better than other base learners in the GNSS NLOS detection tasks [11]. In particular, similar to [11], we adopt the linear SVM classifier, which is trained to find the optimal separating hyperplane to classify inputs into two different categories. Given the training dataset $\boldsymbol{D}_t$, the SVM model can be trained to solve the following optimization problem:

$$\min_{\mathbf{w},b} \frac{1}{2}\|\mathbf{w}\|^2 \tag{1}$$

$$\text{s.t.} \quad (2y_t - 1)((\mathbf{f}_t/\sigma)^T\mathbf{w} + b) \geq 1 \tag{2}$$

where parameters $\sigma \in \mathbf{R}$, $\mathbf{w} \in \mathbf{R}^9$, and $b \in \mathbf{R}$ are the kernel scale, the vector of fit linear coefficients, and the bias of the linear SVM classification, respectively.

When the SVM model is trained to convergence, we can obtain the model parameters $\tilde{\mathbf{w}} \in \mathbf{R}^9$ and $\tilde{b} \in \mathbf{R}$. Then, given an input measurement feature vector $\mathbf{f}_e$ for evaluation, the score of the linear SVM classification is calculated by

$$S_{\text{SVM}}(\mathbf{f}_e) = (\mathbf{f}_e/\sigma)^T\tilde{\mathbf{w}} + \tilde{b}. \tag{3}$$

The value range of the score in (3) is $\{-\infty, \infty\}$, while the prediction results of other base classifiers in the proposed SEL could be positive probabilities. To make the prediction results of different base learners to be consistent, the probabilities that over NLOS of the SVM classification are handled by sigmoid normalizing, that is,

$$p_{\text{SVM}}(\mathbf{f}_e) = \frac{e^{S_{\text{SVM}}(\mathbf{f}_e)}}{1 + e^{S_{\text{SVM}}(\mathbf{f}_e)}}. \tag{4}$$

With (4), the score of the linear SVM classification is normalized to $\{0, 1\}$. In our experiments, we find that the normalization of SVM score is required for training.

First-Level Model ②—XGBoost: The boosting method GBDT [15] or its improved version XGBoost [34] has proved to be a fast and accurate way in GNSS NLOS detection and achieved the state-of-the-art results on various classification tasks. It is an ensemble of tree-based methods that applies the principle of boosting weak learners to improve the final prediction accuracy. The boosting method is an ensemble model by itself but it can still benefit if it is ensemble with other models [32]. In the proposed SEL method, we adopt XGBoost as a base learner to obtain a stronger model for GNSS NLOS detection.

The XGBoost method applies several base models, e.g., classification and regression trees (CARTs), as weak learners and then creates ensemble trees to boost the performance via optimizing a regularized objective function [34]. It is trained in an additive way: the ensemble sequentially adds weak learners that learn from the residual of the previous ensemble. Given the training dataset $\boldsymbol{D}_t$ consists of

Fig. 2. Eight static locations (in orange) and one moving trajectory (in yellow) for GNSS data collection in Hong Kong urban canyon (around latitude 22.299° and longitude 114.177°).

feature-label pairs $\{\mathbf{f}_t, y_t\}$, the ith regularized objective function of the additive training method can be denoted as

$$L_i = \sum_{\{\mathbf{f}_t, y_t\} \in \boldsymbol{D}_t} l(y_t, G_{i-1}(\mathbf{f}_t) + g_i(\mathbf{f}_t)) + \Omega(g_i) \tag{5}$$

where $g_i(\cdot)$ is the weak learners at the ith boosting round, $G_{i-1}(\cdot) = \sum_{k=0}^{i} g_k(\cdot)$ is the ensemble at the (i-1)th boosting round, $l(\cdot)$ is the log-likelihood loss function between the label y_t and the models' prediction output, and $\Omega(\cdot)$ is the regularization function to penalize model complexity of the weak learners g_i of XGBoost.

After the additive training is terminated, output $G_I(\cdot)$ as the final classifier, where I is the number of boosting rounds. Given an input measurement feature vector $\mathbf{f}_e$ for evaluation, the probabilities of NLOS of the XGBoost classification can be obtained as

$$p_{\text{XGBoost}}(\mathbf{f}_e) = G_I(\mathbf{f}_e). \tag{6}$$

Second-Level Model—LR: The LR method is a simple but effective classifier, which is usually adopted to the ensemble learning framework. It is trained to improve the system's final decision based on the prediction of each individual model in the first level. The objective function for training is the log-likelihood function

$$L_{\text{LR}} = \sum_{\{\mathbf{o}_t, y_t\} \in \boldsymbol{D}_t} \left[y_t(\mathbf{o}_t^T \mathbf{u} + v) - \log(1 + e^{\mathbf{o}_t^T \mathbf{u} + v}) \right] \tag{7}$$

where $\mathbf{o}_t = [p_{\text{SVM}}(\mathbf{f}_t), p_{\text{XGBoost}}(\mathbf{f}_t)] \in \mathbf{R}^2$ is the concatenated predictions of the individual models in the first level associated with the training features $\mathbf{f}_t$, and $\mathbf{u} \in \mathbf{R}^2$ and $k \in \mathbf{R}$ are the weight and the bias of the LR method to be trained.

In the process of evaluation, the probabilities of NLOS of the LR method are obtained as

$$p_{\text{LR}}(\mathbf{o}_e) = \frac{e^{\mathbf{o}_e{}^T \tilde{\mathbf{u}} + \tilde{v}}}{1 + e^{\mathbf{o}_e{}^T \tilde{\mathbf{u}} + \tilde{v}}} \tag{8}$$

where $\mathbf{o}_e = [p_{\text{SVM}}(\mathbf{f}_e), p_{\text{XGBoost}}(\mathbf{f}_e)] \in \mathbf{R}^2$ is the concatenated predictions of the individual models in the first level associated with the evaluation features $\mathbf{f}_e$, and $\tilde{\mathbf{u}} \in \mathbf{R}^2$ and $\tilde{v} \in \mathbf{R}$ are the weight and the bias of the LR model that has already been trained.

Finally, the predicted probabilities of NLOS $p_{\text{LR}}(\mathbf{o}_e)$ need to be rounded to the closest value of 1 or 0 to output the NLOS predictions.

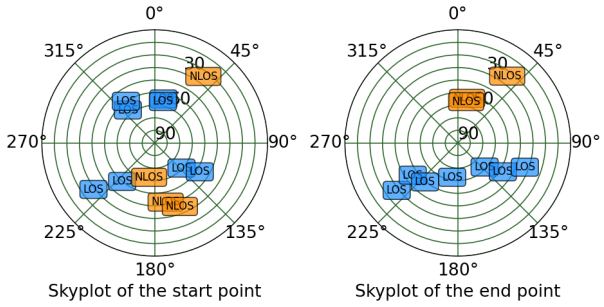

Fig. 3. Sky plot of the start point and endpoint in the moving trajectory with the satellite visibility labeled from ground truth.

III. Results and Discussion

In this section, three separate experiments on real GNSS data derived from urban canyons are designed to test the effectiveness of the proposed SEL method for GNSS NLOS detection. The first experiment is to compare different choices of the individual models in the proposed SEL method. The second one is to evaluate the performance of the proposed method compared with the baseline methods in an in-domain scenario associated with evenly random sampling. The final experiment is to test the generalization performance of the proposed method compared with the existing methods in out-domain scenarios associated with different reception locations and states of motion, respectively.

A. Experimental Setup

1) Data Preparation: In our experiments, two public real datasets[2] of GNSS receivers in urban canyons are used (see Fig. 2): 1) static data—dataset collected at eight different static locations via a UBLOX NEO M8T receiver at different time in June 2018 [11] and 2) dynamic data—dataset collected over a trajectory (about 500 meters) via the moving receiver in May 2021 [37]. With 1-Hz sampling rate, the time duration of each static point is about 20 min and is about 90 s for the dynamic data. In particular, the ground truth location and the surrounding 3-D building model of each sample are processed to obtain the NLOS or LOS label for the datasets [11]. The examples of the sky plot of the dynamic and static data are shown in Figs. 3 and 4, respectively. As the GNSS observations vary over time, the sky plot of each static receiver is plotted based on the last epoch, and the sky plot of the start and end epoches for the moving receiver is plotted. Also, the proportions of NLOS and LOS signals in each dataset are counted (see Figs. 5 and 6). The sky plots and NLOS/LOS proportions show that the reception environments are quite

[2]The datasets are downloaded from the website of Intelligent Positioning and Navigation Laboratory (IPNL): https://www.polyu-ipn-lab.com/

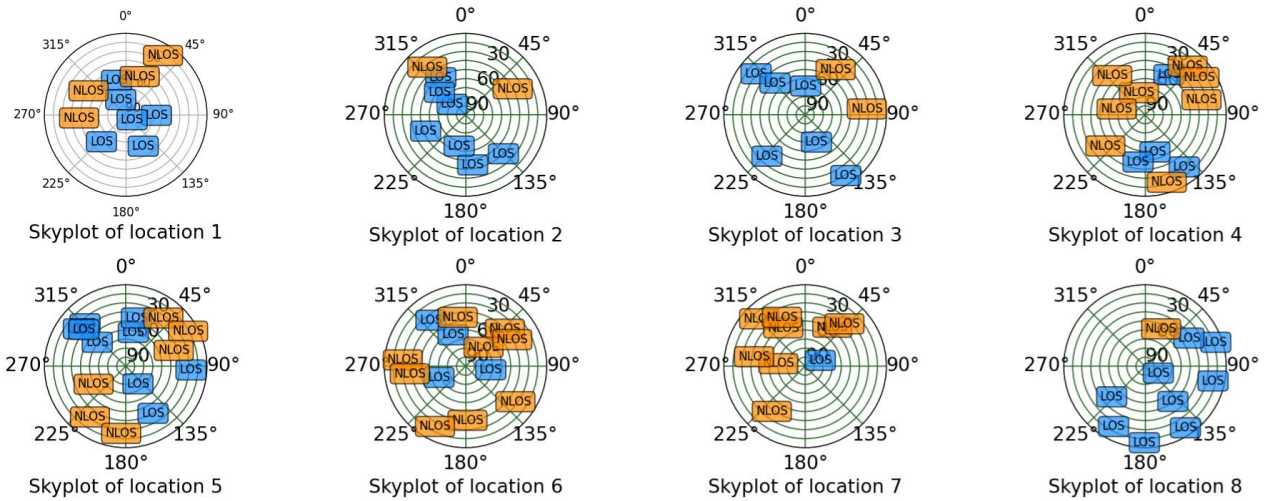

Fig. 4. Sky plot of different static locations with the satellite visibility labeled from ground truth.

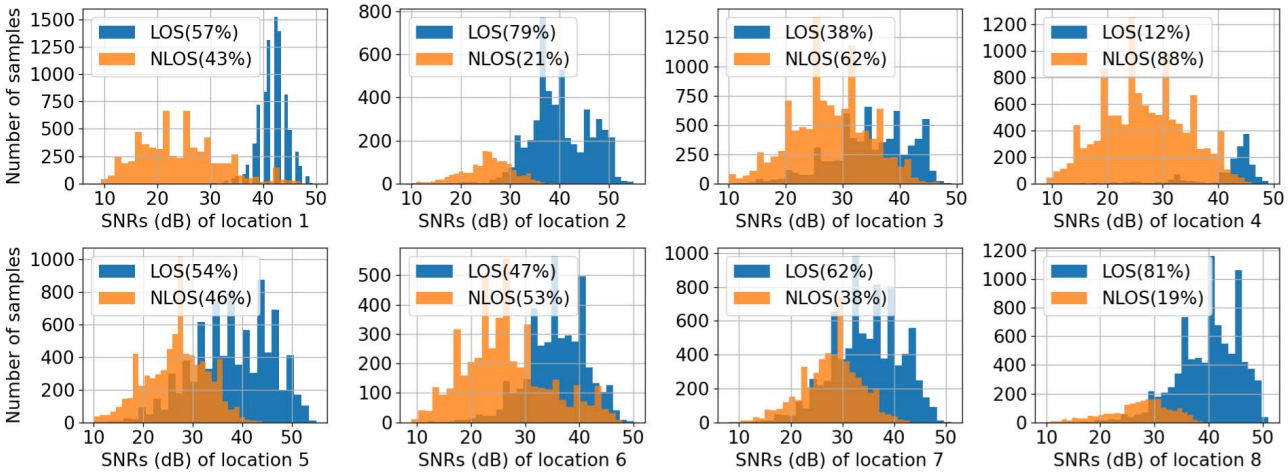

Fig. 5. SNR distributions and NLOS/LOS proportions in different static locations.

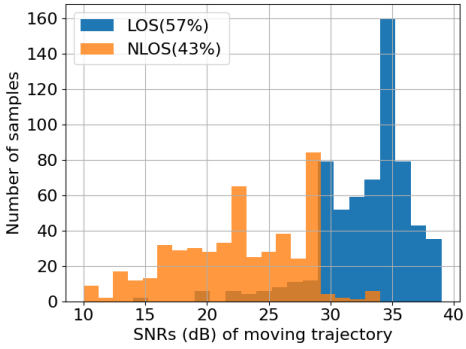

Fig. 6. SNR distributions and NLOS/LOS proportions in the moving trajectory.

different for the datasets. The data at each sampling time are pre-processed to obtain the measurement features in Table I.

To evaluate the performance of the proposed method in different settings, the GNSS data are split into training datasets and evaluation datasets in two manners. First, we randomly select a subset of the collected data samples as the training set and use the remaining samples as the test set to obtain optimal first/second-level models. Second, considering the performance of NLOS detection is usually highly related to the surrounding environment, we also test the generalization of our proposed method in environments that are unseen to the model during training. In particular, we split the dataset into training datasets and evaluation datasets derived from different locations and states of motion, respectively. The details about the experimental scenarios are listed as follows.

1) *In-Domain Scenario* $\mathcal{I}$: All of the data samples, collected at the eight static locations, are mixed together. Then, 90% of the samples are randomly selected for model training, and the 10% remaining are used for evaluation.
2) *Out-Domain Static Scenario*: Among the data samples collected at the eight static locations, we select the samples of the arbitrary seven locations out of the eight locations for model training and then use the remaining one location for model evaluation. Thus, we can

TABLE II

ACCURACY RATES AND COMPUTATIONAL COSTS OF DIFFERENT STRATEGIES FOR MODEL SELECTION ON THE IN-DOMAIN SCENARIO $\mathcal{I}$, THE MEAN VALUE OF THE STATIC OUT-DOMAIN SCENARIO $\mathcal{O}^*$, AND THE OUT-DOMAIN DYNAMIC SCENARIO $\mathcal{D}$, WITH "✓" THE MODEL SELECTION AND "×" THE MODEL IS NOT USED

Strategy	First Level			Second Level		Accuracy Rate			Computational Cost
	SVM	XGBoost	RF	LR	XGBoost	$\mathcal{I}$	$\mathcal{O}^*$	$\mathcal{D}$	
1	×	✓	✓	✓	×	83.55%	76.21%	73.87%	**23 ms**
2	×	✓	✓	×	✓	82.16%	75.11%	73.26%	**27 ms**
3	✓	×	✓	✓	×	87.57%	82.51%	80.86%	39 ms
4	✓	×	✓	×	✓	85.60%	80.29%	78.93%	47 ms
5	✓	✓	×	✓	×	**89.24%**	**85.11%**	**83.80%**	42 ms
6	✓	✓	×	×	✓	88.52%	84.93%	82.52%	51 ms
7	✓	✓	✓	✓	×	**89.71%**	**85.55%**	**84.16%**	56 ms
8	✓	✓	✓	×	✓	88.58%	84.71%	83.19%	61 ms

obtain eight experimental scenarios denoted as $\mathcal{O}_i$, with $i \in \{1, \ldots, 8\}$.

3) *Out-Domain Dynamic Scenario* $\mathcal{D}$: All samples collected at the eight static locations are mixed for model training, and the dynamic data are used as the testing set.

2) Methods and Implementation: We compare the proposed SEL method with state-of-the-art NLOS detection methods based on machine learning, including SVM [11], GBDT [15], and RF [38]. We also consider the conventional SNR classification method [12] as a comparison. Similar to [11], the threshold of the SNR classification is set to 35 dB. The SNR distributions of LOS and NLOS in different static locations and the moving trajectory are shown in Figs. 5 and 6, respectively. Note that the measurements of NLOS signals are significantly smaller than that of LOS signals, while the SNR distributions for NLOS and LOS signals are quite different for different datasets. In our experiments, each machine learning model in the proposed SEL method is conducted using default model hyperparameters in scikit-learn [39].

3) Software/Hardware: All of our experiments were conducted using PyCharm software on a PC with a Core i7 CPU (2.93-GHz with 8-GB memory).

B. Models of SEL

The performance of different model selection strategies on GNSS NLOS detection is shown in Table II. Experimental results show that the accuracy rates of strategy 5 (first level: SVM + XGBoost, second level: LR) and strategy 7 (first level: SVM + XGBoost + RF, second level: LR) are similar, which largely outperform other strategies in the in-domain scenario, the out-domain static scenarios, and the out-domain dynamic scenario.

In the results, the more individual models used in the first level, the higher the accuracy rate. The possible reason would be that the SEL method combines various views to the features from different heterogeneous models and improves the NLOS detection performance. However, one can also find that simply increasing the number of models in the first level may sometimes not improve significantly. For example, compared with strategy 5, strategy 7 adds RF in the first level. The average accuracy of the scenarios is only improved by 0.42%, but the computational cost of each sample for testing is relatively increased by 33.3%.

TABLE III

ACCURACY RATES OF DIFFERENT GNSS NLOS DETECTION METHODS ON THE IN-DOMAIN SCENARIO

Method	Accuracy Rate on $\mathcal{I}$
SNR [12]	80.59%
RF [38]	80.65%
GBDT [15]	83.55%
SVM [11]	85.32%
SEL	**89.24%**

Moreover, the importance of each model's impact on the results varies widely. In the first level, the importance of these three candidate models is SVM, XGBoost, and RF from high to low. Numerically, compared with strategy 7, strategy 1 (strategy 3 or strategy 5) removes SVM (XGBoost or RF), while the average accuracy rate decreases 8.60% (2.82% or 0.42%). In the second level, the performance of LR consistently outperforms XGBoost in terms of accuracy rate and computational cost. Compared with XGBoost, LR is more simple and efficient in the second level. Moreover, the properties of LR and the first layer models are more heterogeneous, which might help the model learn from ensemble features.

In summary, to make a balance between the accuracy rate and the computational cost, we select strategy 5 as the models of the proposed SEL method.

C. Results of the In-Domain Scenario

To evaluate the performance of model training, we design the in-domain scenario and use the pre-split training dataset for model optimization. Then, we test the models' performance on the test dataset. The accuracy rate and the confusion matrix on the in-domain scenario are shown in Tables III and IV, respectively.

In Table III, our experimental results of the in-domain scenario show that the proposed SEL method achieves a very significant performance improvement compared with the baseline methods. The existing methods based on machine learning [11], [15], [38] outperform the traditional SNR

TABLE IV
CONFUSION MATRIX OF DIFFERENT GNSS NLOS DETECTION METHODS ON THE IN-DOMAIN SCENARIO

Method	SNR [12]		RF [38]		GBDT [15]		SVM [11]		SEL	
Label / **Prediction**	NLOS	LOS	NLOS	LOS	NLOS	LOS	NLOS	LOS	NLOS	LOS
NLOS	79.65%	18.49%	79.71%	18.43%	82.61%	15.53%	84.38%	13.76%	88.30%	9.84%
LOS	20.35%	81.51%	20.29%	81.57%	17.39%	84.47%	15.62%	86.24%	11.70%	90.16%

TABLE V
ACCURACY RATES OF DIFFERENT GNSS NLOS DETECTION METHODS ON THE OUT-DOMAIN SCENARIOS

Method	$\mathcal{O}_1$	$\mathcal{O}_2$	$\mathcal{O}_3$	$\mathcal{O}_4$	$\mathcal{O}_5$	$\mathcal{O}_6$	$\mathcal{O}_7$	$\mathcal{O}_8$	$\mathcal{O}^*$	$\mathcal{D}$
SNR [12]	92.50%	79.02%	70.75%	63.74%	69.52%	75.31%	75.50%	82.64%	76.12%	73.16%
RF [38]	93.14%	81.68%	74.14%	63.51%	70.95%	75.64%	78.44%	83.65%	77.64%	74.06%
GBDT [15]	92.76%	83.45%	80.43%	68.08%	72.17%	77.96%	80.26%	85.48%	80.07%	78.35%
SVM [11]	**94.88**%	85.67%	78.13%	72.56%	74.69%	80.15%	83.23%	88.65%	82.25%	80.94%
SEL	94.23%	**87.79**%	**83.89**%	**75.45**%	**77.26**%	**84.66**%	**86.84**%	**90.75**%	**85.11**%	**83.80**%

method [12], while the SVM method is the best one. Xu *et al.* [11] and Zhang *et al.* [16] also found the same results. Although the GBDT method or the RF method is weaker than the SVM method when used alone in NLOS detection tasks, it can still benefit the SEL methods when combining these individuals together. In the experiments, the proposed SEL method consists of the SVM model and the XGBoost model (a type of improved GBDT) in the first level and the LR model in the second level. Compared with the baseline method that adopts SVM [11], GBDT [15], or RF [38] alone, the proposed SEL method improves the accuracy rate of GNSS NLOS detection by 3.92%, 5.69%, and 8.59%, respectively. Moreover, the values of the confusion matrix also show that the proposed SEL method consistently outperforms the baseline machine learning methods in the GNSS NLOS detection tasks (see Table IV).

D. Results of the Out-Domain Scenarios

To evaluate the generalization of the proposed SEL method, two kinds of out-domain scenarios are designed to test the performance on the environment that the model does not see during training. The accuracy rate and the confusion matrix on the out-domain static scenario and out-domain dynamic scenario (see Tables V and VI, respectively) are discussed as follows.

1) Out-Domain Static Scenario: As shown in Table V, the proposed SEL method shows a strong performance compared with the baseline methods on the out-domain static scenarios. In particular, the proposed SEL achieves the highest accuracy rates in seven ($\mathcal{O}_i$, with $i \in \{2, \ldots, 8\}$) of the eight experimental settings, while the performance on $\mathcal{O}_1$ is comparable with the best result of SVM [11]. On average of the accuracy rates in the out-domain static scenarios (i.e., $\mathcal{O}^*$), the proposed SEL method significantly outperforms the baseline methods, including the SNR method [12], SVM [11], GBDT [15], and RF [38] by 8.99%, 2.86%, 5.04%, and 7.47%, respectively. Also, the confusion matrix in Table VI shows that the proposed SEL method has a good generalization performance for different environments, with high detection accuracy and low false detection.

2) Out-Domain Dynamic Scenario: Merely for brevity, the results of our method on the out-domain dynamic scenario are presented in the last column of Tables V and VI. The results indicate that the proposed SEL method achieves the best accuracy rate when compared with the existing methods. Numerically, it outperforms the methods of SNR [12], SVM [11], GBDT [15], and RF [38] by 10.64%, 2.86%, 5.45%, and 9.74%, respectively. Although trained on static data completely, our SEL method does not suffer from large performance degradation when evaluated on the dynamic dataset. A possible reason is that our method is conducted on the measurement features of each epoch, which is not very sensitive to the dynamic features caused by receiver moving. In our future work, more dynamic dataset will be collected for model training to improve the performance on realistic applications.

E. Qualitative Analysis

To further evaluate the effectiveness of our method, we analyze the results from the following two perspectives.

First, the time series of accuracy rates for our SEL method is plotted to qualitatively assess the performance stability (see Fig. 7 for the out-domain static scenarios, and Fig. 8 for the out-domain dynamic scenario). The results of each experimental scenario show that the performance of SEL over different epochs varies within a certain range. Numerically, the standard deviation of the accuracy rate ranges from 5.53 to 13.58 points in the experimental scenarios. A possible reason for the larger variances is the surrounding environment the receiver is located in. For example, $\mathcal{O}_4$ exhibits the largest standard deviation (13.58 points) and the lowest average accuracy (75.45%) than other experimental scenarios. It might be caused by the highest NLOS proportion in $\mathcal{O}_4$ (88%, see Fig. 5), which indicates a much challenging reception environment to the receiver. Conversely, $\mathcal{O}_1$ and $\mathcal{O}_8$ achieve the smallest two standard deviations (5.53 and 8.19 points) and the highest two accuracy rates (94.23% and 90.75%). The reason might be that the two scenarios are simple for NLOS detection tasks with low NLOS proportions (43% and 19%) or easily distinguishable SNR measurements

TABLE VI
CONFUSION MATRIX OF THE PROPOSED SEL METHOD ON THE OUT-DOMAIN SCENARIOS

Method (SEL)	$\mathcal{O}_1$		$\mathcal{O}_2$		$\mathcal{O}_3$		$\mathcal{O}_4$		$\mathcal{O}^*$	
Prediction \ Label	NLOS	LOS	NLOS	LOS	NLOS	LOS	NLOS	LOS	NLOS	LOS
NLOS	93.29%	4.85%	86.85%	11.28%	82.95%	15.19%	74.51%	23.63%	84.37%	14.11%
LOS	6.71%	95.15%	13.15%	88.72%	17.05%	84.81%	25.49%	76.37%	15.63%	85.89%
Method (SEL)	$\mathcal{O}_5$		$\mathcal{O}_6$		$\mathcal{O}_7$		$\mathcal{O}_8$		$\mathcal{D}$	
Prediction \ Label	NLOS	LOS	NLOS	LOS	NLOS	LOS	NLOS	LOS	NLOS	LOS
NLOS	76.32%	21.82%	83.72%	14.41%	85.90%	12.24%	89.81%	8.33%	83.21%	15.60%
LOS	23.68%	78.18%	16.28%	85.59%	14.10%	87.76%	10.19%	91.67%	16.79%	84.40%

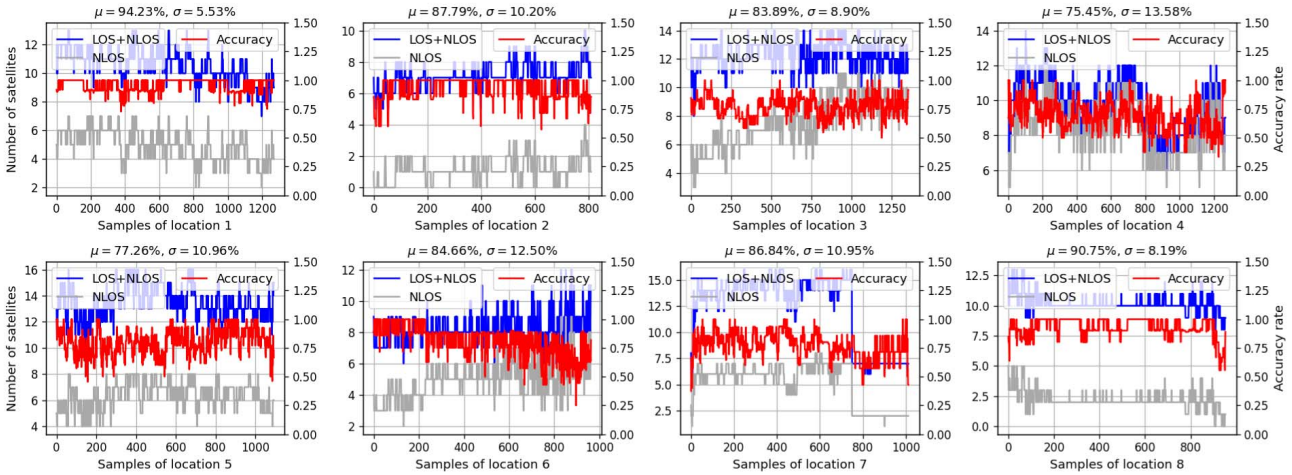

Fig. 7. Number of visible LOS and NLOS, and accuracy rates in time series for the out-domain static scenarios.

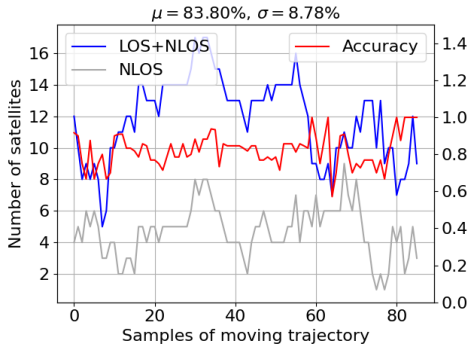

Fig. 8. Number of visible LOS and NLOS, and accuracy rates in time series for the out-domain dynamic scenario.

(see Fig. 5). Regarding the time series of performance on the dynamic data, our SEL method still achieves relatively stable accurate rates even for a moving receiver in urban canyons (see Fig. 8).

Besides the time series analysis on each epoch with only about ten observed satellites (might cause statistical error), we also analyze how the performance of our method changes as the proportions of NLOS signals in different static locations increase. Combining the results from Fig. 5 and Table V, the proportion of NLOS signals is negatively correlated with the accuracy rate of our SEL method. For example, among the top five ($\mathcal{O}_1$, $\mathcal{O}_3$, $\mathcal{O}_4$, $\mathcal{O}_5$, and $\mathcal{O}_6$) of the eight static datasets in terms of NLOS proportion, the accuracy rates for the four datasets ($\mathcal{O}_3$, $\mathcal{O}_4$, $\mathcal{O}_5$, and $\mathcal{O}_6$) are significantly below the average performance ($\mathcal{O}^*$). Numerically, the correlation between the NLOS proportion for each location and accuracy rate is -0.694, which shows a strong negative correlation. We infer that as a larger proportion of NLOS signals usually indicates a more complex reception environment, the method may suffer from issues of performance degradation for a large NLOS proportion.

IV. CONCLUSION

In this article, a novel stacking-based ensemble learning method has been proposed for the NLOS detection of GNSS. It combines different machine learning methods from different views to address the shortcomings of each single model. The proposed method effectively leveraged the existing individual machine learning models to enhance NLOS detection for GNSS applications, and significantly improved the performance on real GNSS data compared with the baseline methods.

In the future, features of other sensors, such as fish-eye cameras and LiDARs, will be included in the proposed SEL method. Also, ensemble deep learning will be researched for GNSS NLOS detection to obtain better generalization performance.

ACKNOWLEDGMENT

The authors would like to thank Haosheng Xu and Li-Ta Hsu for sharing the real global navigation satellite system data and constructive suggestions for this work.

REFERENCES

[1] N. Dasanayaka and Y. Feng, "Analysis of vehicle location prediction errors for safety applications in cooperative-intelligent transportation systems," *IEEE Trans. Intell. Transp. Syst.*, early access, Jan. 20, 2022, doi: 10.1109/TITS.2022.3141710.

[2] S. Y. Cho and W. S. Choi, "Robust positioning technique in low-cost DR/GPS for land navigation," *IEEE Trans. Instrum. Meas.*, vol. 55, no. 4, pp. 1132–1142, Aug. 2006.

[3] A. Ul Haque, T. Mahmood, and M. Saeed, "Enhanced GNSS positioning solution on Android for location based services using big data," *J. Internet Technol.*, vol. 20, no. 2, pp. 399–407, 2019.

[4] Y. Sun, "Autonomous integrity monitoring for relative navigation of multiple unmanned aerial vehicles," *Remote Sens.*, vol. 13, no. 8, p. 1483, Apr. 2021.

[5] B. Xu, Q. Jia, and L.-T. Hsu, "Vector tracking loop-based GNSS NLOS detection and correction: Algorithm design and performance analysis," *IEEE Trans. Instrum. Meas.*, vol. 69, no. 7, pp. 4604–4619, Jul. 2020.

[6] J. Bressler, P. Reisdorf, M. Obst, and G. Wanielik, "GNSS positioning in non-line-of-sight context—A survey," in *Proc. IEEE 19th Int. Conf. Intell. Transp. Syst. (ITSC)*, Nov. 2016, pp. 1147–1154.

[7] P. Francois, B. David, and M. Florian, "Non-line-of-sight GNSS signal detection using an on-board 3D model of buildings," in *Proc. 11th Int. Conf. ITS Telecommun.*, Aug. 2011, pp. 280–286.

[8] Z. Lyu and Y. Gao, "A new method for non-line-of-sight GNSS signal detection for positioning accuracy improvement in urban environments," in *Proc. 33rd Int. Tech. Meeting Satell. Division Inst. Navigat. (ION GNSS+)*, Oct. 2020, pp. 2972–2988.

[9] S. Haigh, J. Kulon, A. Partlow, P. Rogers, and C. Gibson, "A robust algorithm for classification and rejection of NLOS signals in narrowband ultrasonic localization systems," *IEEE Trans. Instrum. Meas.*, vol. 68, no. 3, pp. 646–655, Aug. 2018.

[10] P. Xie and M. G. Petovello, "Measuring GNSS multipath distributions in urban canyon environments," *IEEE Trans. Instrum. Meas.*, vol. 64, no. 2, pp. 366–377, Feb. 2015.

[11] H. Xu, A. Angrisano, S. Gaglione, and L.-T. Hsu, "Machine learning based LOS/NLOS classifier and robust estimator for GNSS shadow matching," *Satell. Navigat.*, vol. 1, no. 1, pp. 1–12, Dec. 2020.

[12] L. Wang, P. D. Groves, and M. K. Ziebart, "Smartphone shadow matching for better cross-street GNSS positioning in urban environments," *J. Navigat.*, vol. 68, no. 3, pp. 411–433, 2015.

[13] D. H. Won *et al.*, "Weighted DOP with consideration on elevation-dependent range errors of GNSS satellites," *IEEE Trans. Instrum. Meas.*, vol. 61, no. 12, pp. 3241–3250, Dec. 2012.

[14] L.-T. Hsu, "GNSS multipath detection using a machine learning approach," in *Proc. IEEE 20th Int. Conf. Intell. Transp. Syst. (ITSC)*, Oct. 2017, pp. 1–6.

[15] R. Sun, G. Wang, W. Zhang, L.-T. Hsu, and W. Y. Ochieng, "A gradient boosting decision tree based GPS signal reception classification algorithm," *Appl. Soft Comput.*, vol. 86, Jan. 2020, Art. no. 105942.

[16] G. Zhang, B. Xu, and L.-T. Hsu, "GNSS shadow matching based on intelligent LOS/NLOS classifier," in *Proc. 16th IAIN World Congr.*, 2018, pp. 1–7.

[17] S. Kato, M. Kitamura, T. Suzuki, and Y. Amano, "Nlos satellite detection using a fish-eye camera for improving GNSS positioning accuracy in urban area," *J. Robot. Mechatronics*, vol. 28, no. 1, pp. 31–39, 2016.

[18] J. S. Sánchez, A. Gerhmann, P. Thevenon, P. Brocard, A. B. Afia, and O. Julien, "Use of a FishEye camera for GNSS NLOS exclusion and characterization in urban environments," in *Proc. Int. Tech. Meeting The Inst. Navigat.*, Feb. 2016, pp. 283–292.

[19] W. W. Wen, G. Zhang, and L.-T. Hsu, "GNSS NLOS exclusion based on dynamic object detection using LiDAR point cloud," *IEEE Trans. Intell. Transp. Syst.*, vol. 22, no. 2, pp. 853–862, Feb. 2021.

[20] W. Wen and L.-T. Hsu, "3D LiDAR aided GNSS NLOS mitigation in urban canyons," 2021, *arXiv:2112.06108*.

[21] V. Filippov, D. Tatarnicov, J. Ashjaee, A. Astakhov, and I. Sutiagin, "The first dual-depth dual-frequency choke ring," in *Proc. 11th Int. Tech. Meeting Satell. Division The Inst. Navigat. (ION GPS)*, 1998, pp. 1035–1040.

[22] P. D. Groves, Z. Jiang, M. Rudi, and P. Strode, *A Portfolio Approach to NLOS and Multipath Mitigation in Dense Urban Areas*. Richmond, VA, USA: Institute of Navigation, 2013.

[23] R. D. J. van Nee, J. Siereveld, P. C. Fenton, and B. R. Townsend, "The multipath estimating delay lock loop: Approaching theoretical accuracy limits," in *Proc. IEEE Position, Location Navigat. Symp. (PLANS)*, Apr. 1994, pp. 246–251.

[24] X. Chen, F. Dovis, S. Peng, and Y. Morton, "Comparative studies of GPS multipath mitigation methods performance," *IEEE Trans. Aerosp. Electron. Syst.*, vol. 49, no. 3, pp. 1555–1568, Jul. 2013.

[25] P. D. Groves and Z. Jiang, "Height aiding, C/N0 weighting and consistency checking for GNSS NLOS and multipath mitigation in urban areas," *J. Navigat.*, vol. 66, no. 5, pp. 653–669, Sep. 2013.

[26] S. Tay and J. Marais, "Weighting models for GPS pseudorange observations for land transportation in urban canyons," in *Proc. 6th Eur. Workshop GNSS Signals Signal Process.*, Dec. 2013, p. 4.

[27] L. T. Hsu, Y. Gu, and S. Kamijo, "NLOS correction/exclusion for GNSS measurement using RAIM and city building models," *Sensors*, vol. 15, no. 7, pp. 17329–17349, 2015.

[28] Z. Jiang and P. D. Groves, "GNSS NLOS and multipath error mitigation using advanced multi-constellation consistency checking with height aiding," in *Proc. 25th Int. Tech. Meeting Satell. Division Inst. Navigat. (ION GNSS)*, 2012, pp. 79–88.

[29] Z. Jiang, P. D. Groves, W. Y. Ochieng, S. Feng, C. D. Milner, and P. G. Mattos, "Multi-constellation GNSS multipath mitigation using consistency checking," in *Proc. 24th Int. Tech. Meeting Satell. Division Inst. Navigat. (ION GNSS)*, 2011, pp. 3889–3902.

[30] O. Sagi and L. Rokach, "Ensemble learning: A survey," *WIREs Data Mining Knowl. Discovery*, vol. 8, no. 4, Jul. 2018, Art. no. e1249.

[31] T. G. Dietterich, "Ensemble methods in machine learning," in *Proc. Int. Workshop Multiple Classifier Syst.*, Cham, Switzerland: Springer, 2000, pp. 1–15.

[32] H. Baker, M. R. Hallowell, and A. J.-P. Tixier, "Ai-based prediction of independent construction safety outcomes from universal attributes," *Autom. Construct.*, vol. 118, Oct. 2020, Art. no. 103146.

[33] E. Alickovic and A. Subasi, "Ensemble SVM method for automatic sleep stage classification," *IEEE Instrum. Meas.*, vol. 67, no. 6, pp. 1258–1265, Jun. 2018.

[34] T. Chen and C. Guestrin, "XGBoost: A scalable tree boosting system," in *Proc. 22nd ACM SIGKDD Int. Conf. Knowl. Discovery Data Mining*, Aug. 2016, pp. 785–794.

[35] S. Menard, *Applied Logistic Regression Analysis*, vol. 106. Newbury Park, CA, USA: Sage, 2002.

[36] Y. Sun, "RAIM-NET: A deep neural network for receiver autonomous integrity monitoring," *Remote Sens.*, vol. 12, no. 9, p. 1503, May 2020.

[37] G. Zhang, P. Xu, H. Xu, and L.-T. Hsu, "Prediction on the urban GNSS measurement uncertainty based on deep learning networks with long short-term memory," *IEEE Sensors J.*, vol. 21, no. 18, pp. 20563–20577, Sep. 2021.

[38] M. Ramadan, V. Sark, J. Gutierrez, and E. Grass, "NLOS identification for indoor localization using random forest algorithm," in *Proc. WSA 22nd Int. ITG Workshop Smart Antennas*, 2018, pp. 1–5.

[39] F. Pedregosa *et al.*, "Scikit-learn: Machine learning in Python," *J. Mach. Learn. Res.*, vol. 12, pp. 2825–2830, Jan. 2012.

Yuan Sun received the B.E. degree from the School of Instrumentation Science and OptoElectronics Engineering, Beihang University, Beijing, China, in 2011, and the Ph.D. degree from the School of Electronic and Information Engineering, Beihang University, in 2016.

She is currently a Lecturer with the School of Electronics Engineering, Beijing University of Posts and Telecommunications, Beijing. Her primary research interests include global navigation satellite system positioning and integrity monitoring.

Li Fu received the B.E. degree from the School of Advanced Engineering, Beihang University, Beijing, China, in 2011, and the Ph.D. degree from the School of Electronic and Information Engineering, Beihang University, in 2016.

He is currently an Algorithm Engineer with JD AI Research, Beijing, China. His primary research interests include global navigation satellite system positioning, computer vision, multisensor integration, and intelligent unmanned systems.